Food and Chemical Toxicology 130 (2019) 79–88

Contents lists available at ScienceDirect

Food and Chemical Toxicology

journal homepage: www.elsevier.com/locate/foodchemtox

Human CYP3A4-mediated toxification of the pyrrolizidine alkaloid lasiocarpine

Johanna Ebmeyer[a], Albert Braeuning[a], Hansruedi Glatt[a], Anja These[b], Stefanie Hessel-Pras[a,*,1], Alfonso Lampen[a,1]

[a] German Federal Institute for Risk Assessment, Department Food Safety, Max-Dohrn-Straße 8-10, 10589, Berlin, Germany
[b] German Federal Institute for Risk Assessment, Department Safety in the Food Chain, Max-Dohrn-Straße 8-10, 10589, Berlin, Germany

Keywords:
γH2AX
In vitro metabolism
Micronucleus test
Microsomes
Supersomes
S9

A B S T R A C T

Pyrrolizidine alkaloids (PA) are widely distributed phytotoxins contaminating food and feed. Hepatic enzymes are considered to bioactivate PA. Previous studies showed differences in the metabolism rate in liver homogenates of different species. Thus, uncertainty remains with respect to the relevance of human metabolism. Our study aimed to analyze whether the PA representative lasiocarpine is toxified by human cytochrome P450 (CYP) enzymes.

We compared the metabolic elimination of lasiocarpine in the presence of rat and human S9 fractions and liver microsomes. Experiments with the potent CYP3A/Cyp3a inhibitor ketoconazole and supersomes containing individual human and rat CYPs revealed that enzymes of the CYP3A/Cyp3a family of both species are of major relevance for lasiocarpine metabolism. To assess if metabolism by human CYP3A4 results in a toxification of lasiocarpine we performed experiments with V79 cells. γH2AX and micronucleus formation were analyzed as endpoints for genotoxicity. No effects were observed in the wildtype cells, which lack CYP activity. By contrast, a V79 clone engineered for expression of human CYP3A4 showed concentration-dependent γH2AX and micronucleus formation.

Concluding, our results showed the CYP3A4-dependent formation of genotoxic metabolites of lasiocarpine. The results confirm previous data indicating the need to include metabolism of PA for human risk assessment.

1. Introduction

Pyrrolizidine alkaloids (PA) comprise a large group of secondary metabolites synthesized by a wide variety of plant species as a defense against herbivores. It is estimated that more than 660 PA arise in over 6000 plant species, mainly from the families Asteraceae, Boraginaceae and Fabaceae. Humans, livestock and wildlife are exposed to these substances by uptake of contaminated food and feed.

PA share a common structure based on a 1-hydroxymethylpyrrolizidine (necine base) esterified with aliphatic mono- or dicarboxylic acids (necine acids). They are divided into four different structure types according to their necine base: the 1,2-unsaturated PA of the retronecine-, heliotridine- and otonecine-type, as well as the 1,2-saturated PA of the platynecine-type. The double bond in 1,2-position is required for toxicity. Furthermore, at least one hydroxyl group at the ring system has to be esterified for exerting toxic effects. A branched chain of the acid moiety strengthens the toxicity (Mattocks, 1986). In plants, PA mostly occur as *N*-oxides. The PA *N*-oxides are oxidized at the nitrogen of the necine base and thus are more hydrophilic than their parent congeners. As they can be reduced to free PA, *N*-oxides provide similar toxic effects to those observed with the corresponding parent PA (Wiedenfeld et al., 2008).

Abbreviations: **γH2AX**, phosphorylated histone H2AX; **ACN**, acetonitrile; **ANOVA**, analysis of variance; **BSA**, bovine serum albumin; **CBPI**, cytokinesis block proliferation index; **CTB**, CellTiter-Blue viability assay; **CYP**, cytochrome P450; **DAPI**, 4′,6-diamidino-2-phenylindole; **EMS**, ethyl methanesulfonate; **hLM**, human liver microsomes; **hS9**, human S9; **iRS9**, S9 of a rat pretreated with the CYP-inducers β-naphthoflavone and phenobarbital; **MN**, micronucleus-positive cells; **MoE**, margin of exposure; **nRS9**, S9 of a native, non-pretreated rat; **PA**, pyrrolizidine alkaloid(s); **PBS**, phosphate buffered saline; **PBS-T**, PBS supplemented with 0.1% Tween-20; **rLM**, rat liver microsomes; **S9**, supernatant of a liver homogenate after centrifugation at 9000 × *g*; **V79-hCYP3A4**, human CYP3A4 expressing clone of the Chinese hamster cell line V79; **V79-wt**, wildtype of the Chinese hamster cell line V79

* Corresponding author. German Federal Institute for Risk Assessment, Department Food Safety, Max-Dohrn-Strasse 8-10, 10589, Berlin, Germany.
E-mail address: stefanie.hessel-pras@bfr.bund.de (S. Hessel-Pras).

[1] equally contributed to this work.

https://doi.org/10.1016/j.fct.2019.05.019
Received 18 January 2019; Received in revised form 8 May 2019; Accepted 13 May 2019
Available online 16 May 2019

Several PA congeners are genotoxic, carcinogenic, hepatotoxic or pneumotoxic (Wiedenfeld, 2011). In case studies from Afghanistan and India, people developed veno-occlusive disease as hepatotoxic outcome after ingestion of highly PA-contaminated wheat flour or seeds (Kakar et al., 2010; Tandon et al., 1976). The German Federal Institute for Risk Assessment identified tea and honey as main sources contributing to the human exposure of PA in Western countries (BfR, 2013; Dusemund et al., 2018). Bodi et al. (2014) and Mulder et al. (2018) analyzed samples from the German and European retail and internet market for their PA content. They determined that more than 90% of the analyzed herbal tea samples and more than 70% of the non-herbal tea samples were contaminated with PA. Risk assessment of PA is performed using the margin of exposure (MoE) approach. This approach represents a tool used by risk assessors to consider possible safety concerns arising from genotoxic carcinogens in food and feed (EFSA, 2005). It relates a reference point, representing a dose that causes a low but measurable toxic effect, to the total human exposure. EFSA advised to use the benchmark dose lower confidence limit for a 10% excess cancer risk ($BMDL_{10}$) as the reference point (EFSA, 2005). For PA risk assessment, EFSA derived a $BMDL_{10}$ of 237 μg/kg bw based on a chronic toxicity study conducted in rats with the PA riddelliine with the induction of haemangiosarcomas in livers as the most sensitive endpoint (EFSA, 2017). According to this approach the human exposure via contaminated food may lead to MoE values of < 10 000, especially for consumers of high amounts of these products, and consequently should be considered as a possible concern for human health (BfR, 2016, 2018; EFSA, 2011, 2017).

It is considered that toxicity is not exerted by PA itself but by reactive intermediates formed during hepatic metabolism. The hepatic metabolism of PA is initiated with an oxidation catalyzed by cytochrome P450 mono-oxygenases (CYP) (Fig. 1). The following dehydration results in pyrrolic esters, which are highly reactive and form protein and DNA adducts as well as DNA/protein cross-links. This activation of PA provokes acute toxicity in different organs as well as genotoxicity (Ruan et al., 2014; Wiedenfeld, 2011). Conjugation of the reactive intermediates with glutathione has long been considered to result in enhanced excretion, thus representing a mechanism of detoxification (Ruan et al., 2014). It was shown that PA-induced cytotoxicity is reduced in the presence of glutathione or glutathione precursors (Ji et al., 2009; Neuman et al., 2007). However, results from He et al. (2017) show that PA-derived glutathione adducts can bind to cellular DNA and thus might still have some toxic potential.

Phase I metabolism of PA is often simulated *in vitro* by the use of hepatic liver fractions (S9 fraction and liver microsomes) to analyze toxic effects of PA in cell lines with low endogenous metabolic activity. Both liver fractions are prepared from liver homogenates. The S9 fraction represents the post-mitochondrial supernatant after centrifugation at 9000 × *g* containing cytosolic and microsomal proteins. Liver microsomes (mainly fragments of the endoplasmatic reticulum) are isolated by a second centrifugation separating cytosolic from microsomal proteins. Thus, liver microsomes show higher CYP content than S9 fraction when having the same total protein content.

Previous studies found significant differences in the turnover rate of selected PA by S9 fractions of different species (Kolrep et al., 2018). This raised the question about the relevance of human metabolism for toxification of PA. Thus, our study aimed to analyze if PA are toxified by human enzymes. The degradation of the PA representative lasiocarpine by S9 fraction and liver homogenates of rat, as a species often

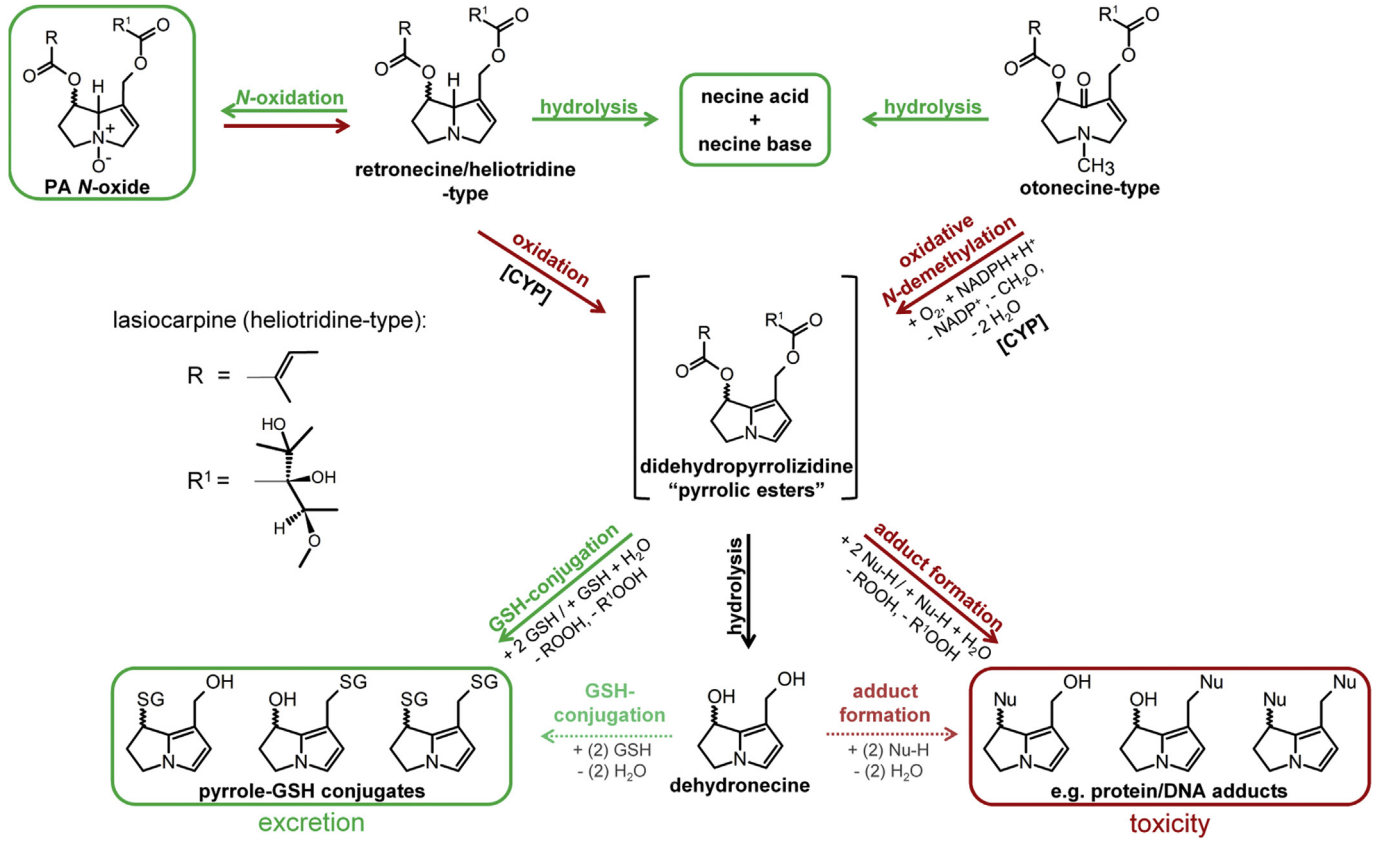

Fig. 1. Overview of PA metabolism. Metabolism of 1,2-unsaturated PA of the retronecine-, heliotridine- or otonecine-type comprises detoxifying (*N*-oxidation, hydrolysis, GSH-conjugation; green) and toxifying (oxidation, oxidative *N*-demethylation; red) reactions. The reactive intermediate didehydropyrrolizidine reacts with nucleophilic centers, e.g. in glutathione (GSH), proteins, or DNA. Oxidation and oxidative *N*-demethylation are supposed to be cytochrome P450 (CYP)-dependent [modified after (Chen et al., 2010; Prakash et al., 1999; Ruan et al., 2014)]. (For interpretation of the references to colour in this figure legend, the reader is referred to the Web version of this article.)

Table 1
Overview of supersomes used in this study.

CYP	CYP content [pmol/mL]	Protein content [mg/mL]	Lot
h1A1	1000	15.0	7104001
h1A2	1000	5.1	5056003
h2A6	1000	2.6	6305002
h2B6	1000	8.9	2142632
h2C8	1000	3.4	7005001
h2C9	1000	4.1	7017001
h2C18	1000	4.8	5301003
h2C19	1000	3.1	6055001
h2D6	1000	8.6	7114001
h3A4	1000	6.8	5322004
h3A5	1000	12.0	5350002
r1a1	2000	3.3	5083004
r1a2	1000	4.0	4072001
r2b1	1000	13.0	28839
r2c6	1000	5.3	6301001
r2c11	1000	5.6	2199986
r2c12	1000	10.0	27951
r2c13	1000	5.1	32808
r2d1	1000	6.7	7052002
r3a1	1000	3.3	607004
r3a2	1000	6.4	4349003

used for *in vivo* studies and *in vitro* metabolism, was compared to those of human hepatic preparations. CYP forms involved were identified. The toxic potential of metabolites formed by human CYP3A4 was analyzed in CYP-deficient V79-wildtype (V79-wt) cells and in V79 stably transfected with human CYP3A4 (V79-hCYP3A4). Hence, effects being clearly CYP3A4-dependent could be observed. Phosphorylation of the histone H2AX (γH2AX formation) and micronucleus induction represented marker endpoints for genotoxicity.

2. Material and methods

2.1. Chemicals

Lasiocarpine (> 98% purity) was purchased from PhytoLab (Vestenbergsgreuth, Germany) and dissolved in 50% acetonitrile (ACN)/50% water (v/v) to obtain stock solutions of 5 mM (metabolism studies) or 250 mM (experiments with V79 cells). ACN and methanol in LC-MS grade were obtained from Merck KGaA (Darmstadt, Germany). All other chemicals for buffers and bioactivation mix were purchased from Sigma Aldrich (Darmstadt, Germany) in the highest purity available.

2.2. In vitro metabolism

2.2.1. In vitro metabolism using liver fractions of rat and human

Hepatic metabolism of lasiocarpine was investigated in different liver fractions (S9 fraction and liver microsomes) of rat and human. Human S9 fraction (hS9), human liver microsomes (hLM) and rat liver microsomes (rLM) were purchased from Corning (Corning, New York, USA). Rat S9 fractions were derived from liver homogenates as described before (Ames et al., 1975) by centrifugation at 9000 × *g*. For induction of xenobiotic metabolizing enzymes, a male Wistar rat was treated daily with β-naphthoflavone (80 mg/kg body weight, oral by gavage) and phenobarbital sodium (80 mg/kg body weight, intraperitoneal) for three days prior to liver isolation to receive induced rat S9 fraction (iRS9) according to the OECD guideline 471. Animals for gaining native rat S9 fraction (nRS9) remained untreated. Experiments with animals for preparing rat S9 fraction were performed according to European laws and with the consent of the responsible authority of the state of Berlin (Regional Office for Health and Social Affairs Berlin—LAGeSo), numbers H0256/02 (treatment of animals) and T0258/02 (killing of animals and removal of organs). Protein contents of the resulting S9 fractions were determined according to Bradford (1976) and adjusted to 20 mg/mL, the same protein content as the purchased liver fractions. The total CYP concentrations of the subcellular liver fractions were determined by measurement of CO-difference spectra as described before (Omura and Sato, 1964) with the following modifications: liver fractions were diluted to a protein content of 1.6–3.0 mg/mL in 0.1 M sodium phosphate buffer (pH 7.4) containing 10% glycerol and 0.05% Triton X-100. Reduction of samples was effected with 50 mM sodium dithionite. After bubbling of the sample with CO absorption spectra (400–500 nm) were recorded. CYP concentration was calculated with the following extinction coefficient: $\varepsilon_{450\text{-}490} = 91\ mM^{-1}$.

A mixture of 4 parts of lasiocarpine solution (12.5 µM) and 1 part of S9 or microsomes activation mix was used for metabolism studies, resulting in a final concentration of 10 µM lasiocarpine with 0.1% ACN and a final protein concentration of 0.4 mg/mL. The activation mix consisted of 33 mM potassium chloride, 8 mM magnesium chloride, 4 mM NADP, 5 mM glucose-6-phosphate and 10% S9 fraction/microsomes diluted in 15 mM sodium phosphate buffer (pH 7.4). Glucose-6-phosphate-dehydrogenase (0.5 U/mL) was added to the mixture for NADPH regeneration for bioactivation experiments with microsomes. Endogenous glucose-6-phosphate-dehydrogenase served as NADPH-regenerating system during bioactivation with S9 mix. The mixture was incubated at 37 °C. Samples were taken for analysis of lasiocarpine content (section 2.2.3) after 0.5, 1, 2 and 4.5 h and transferred to methanol to stop the reaction, resulting in a dilution of the initial concentration of 10 µM lasiocarpine to 714 nM (dilution factor of 14). The experiment was additionally repeated in the presence of 8 µM ketoconazole, which represents a potent CYP3A/Cyp3a inhibitor (Baldwin et al., 1995; Maurice et al., 1992), to assess if enzymes of the CYP3A/CYP3a family play a role in lasiocarpine metabolism. The concentration of 8 µM ketoconazole was shown before to be efficient in CYP3A/Cyp3a inhibition (Eagling et al., 1998).

2.2.2. In vitro metabolism using recombinant human and rat microsomes (supersomes)

In order to identify specific CYP forms involved in the metabolism of lasiocarpine, metabolism experiments were performed using recombinant enzymes prepared from insect cells infected with baculovirus containing cDNA (supersomes) of different human or rat CYP enzymes with potential relevance for PA metabolism: human CYP1A1, 1A2, 2A6, 2B6, 2C8, 2C9, 2C18, 2C19, 2D6, 3A4, 3A5, and rat Cyp1a1, 1a2, 2b1, 2c6, 2c11, 2c12, 2c13, 2d1, 3a1 and 3a2. All supersomes were purchased from Becton Dickinson (Heidelberg, Germany) or Corning (Corning, New York, USA) and are listed in Table 1. Insect control supersomes (Corning) served as control for CYP-independent metabolism.

Metabolism studies were performed as described for S9 and microsomes mix in section 2.2.1 with a CYP content of 40 pmol/mL or 4% insect control supersome. Glucose-6-phosphate dehydrogenase (0.5 U/mL) was added for regeneration of NADPH.

2.2.3. Sample preparation and LC-MS/MS analysis of lasiocarpine

Lasiocarpine content of metabolism samples was analyzed by LC-MS/MS. Samples from metabolism studies in methanol were centrifuged at 12 000 × *g* for 10 min at 4 °C to precipitate the protein. A seven-point calibration curve covering a concentration range from 1 to 1000 nM lasiocarpine was used for quantification. Remaining unchanged lasiocarpine in the cell culture supernatant was referred to the initial concentration of 10 µM lasiocarpine (t = 0 h), analyzed using a solution of 10 µM non-metabolized lasiocarpine diluted in the same way as the metabolism samples.

Reversed phase separation was achieved on a 150 × 2.1 mm; 1.9 µm C18 Hypersil Gold column with guard protection (Thermo Fisher, Runcorn, UK) at a flow rate of 0.3 mL/min on an UltiMate 3000 (Thermo Scientific, Germany) UHPLC system as described before

(Kolrep et al., 2018).

2.3. Cell culture

V79-Mz cells are control V79 cells maintained in the laboratory of Prof. Dr. Glatt in Mainz and then in Potsdam. They were the recipient cell for the construction of CYP-expressing cell lines. Therefore, they were used here as wildtype control cells (V79-wt). V79-Mz cells were analyzed for various activities of xenobiotic metabolizing enzymes before and found to be deficient in the expression of CYPs, sulfotransferases and UDP-glucuronosyltransferases (Glatt et al., 1990; Liu et al., 2016). This cell line was genetically engineered for expression of human CYP3A4 and human NADPH-CYP oxidoreductase, which enhances CYP3A4 metabolic activity, as described before (Schneider et al., 1996) and is termed in this paper as V79-hCYP3A4. For analysis of phosphorylation of the histone H2AX (γH2AX formation), both cell lines were cultured in high-glucose Dulbecco's modified Eagle medium (PAN-Biotech, Aidenbach, Germany) supplemented with 5% fetal bovine serum (Capricorn Scientific, Ebsdorfergrund, Germany), 100 U/mL penicillin and 100 µg/mL streptomycin (Capricorn Scientific) at 37 °C in a humidified atmosphere of 5% CO_2. For the micronucleus test, cells were maintained in minimal essential medium (Capricorn Scientific) supplemented with 10% fetal bovine serum (Capricorn Scientific), 100 U/mL penicillin and 100 µg/mL streptomycin (Capricorn Scientific).

2.4. Cell viability

To analyze if human CYP3A4 converts lasiocarpine to cytotoxic metabolites cell viability of lasiocarpine-treated V79-wt and V79-hCYP3A4 cells was analyzed via DNA quantification by 4′,6-diamidino-2-phenylindole (DAPI) staining and CellTiter-Blue cell viability assay (CTB; Promega, Madison, USA). Thus, 2×10^5 cells/well were seeded in a 96-well plate und cultivated for 1 day. Afterwards, cells were treated with 1–500 µM lasiocarpine. ACN (0.2%) was used as a solvent control. Triton X-100 (0.01%) served as a metabolism-independent positive control for cytotoxicity. Aflatoxin B1 (0.01–1 µM), which is converted to cytotoxic metabolites by human CYP3A4, was used as metabolism-dependent positive control. After 23.5 h of incubation 20 µL of diluted CTB reagent [1:4 phosphate-buffered saline (PBS; 137 mM NaCl, 2.7 mM KCl, 10 mM Na_2HPO_4, 1.8 mM KH_2PO_4, pH 7.4)] was added to the cells and incubated for further 30 min at 37 °C prior to measuring the fluorescence intensity in a Tecan Infinite M200 Pro spectrophotometer (540Ex/590 Em). Afterwards, the supernatant was discarded, cells were fixed with ice-cold methanol for 30 min at room temperature and DAPI solution [3 µM in PBS] was added. DAPI fluorescence intensity was measured in the Tecan Infinite M200Pro spectrophotometer (380Ex/460 Em) after another 30 min of incubation.

The analysis of cell viability in V79-hCYP3A4 was repeated in the presence of 5 µM of the potent CYP3A inhibitor ketoconazole to assess whether the sensitivity of V79-hCYP3A4 cells towards lasiocarpine is CYP3A4-dependent. The concentration of 5 µM ketoconazole was shown before to be efficient in CYP3A4 inhibition (Eagling et al., 1998).

2.5. Qualitative microscopic analysis of γH2AX formation

Phosphorylation of the histone H2AX, then called γH2AX, was qualitatively analyzed microscopically after immunostaining. Thus, 6×10^5 cells were seeded on a cover slip in a 24-well plate and treated after 1 day of cultivation with 1–300 µM lasiocarpine for 24 h. Doxorubicin (0.25 µM) as a double-strand break-inducing substance served as metabolism-independent positive control. Aflatoxin B1 was used as a metabolism-dependent positive control at a concentration of 0.1 µM. The supernatant was removed and cells were fixed with ice cold methanol for 30 min at room temperature. Methanol was discarded and cells were washed with PBS supplemented with 0.1% Tween-20 (PBS-T; Sigma Aldrich, Darmstadt, Germany) for 2 min before blocking with 1% bovine serum albumin (BSA) in PBS-T for 1 h at room temperature. Blocking solution was removed and cells were washed with PBS-T prior to incubation with primary anti-γH2AX antibody [anti-phospho-histone H2A.X (Ser139), clone JBW301, Merck, Darmstadt, Germany, 1:500 in 1% BSA in PBS-T] for 1 h at room temperature. Incubation with secondary antibody [Alexa Fluor 633, F(ab')2-Goat anti-Mouse IgG (H + L), Invitrogen, Fisher scientific, Newington, New Hampshire, USA, 1:400 in 1% BSA in PBS-T] followed after three times of washing with PBS-T. The secondary antibody was removed, cells were washed three times for 2 min with PBS-T before incubation with SYTOX Orange nucleic acid stain (Life Technologies, Carlsbad, California, USA, 1:5000 in PBS-T) for 30 min at room temperature. Staining solution was removed and cells were washed two times with PBS-T, dehydrated with 70% ethanol followed by washing with 98% ethanol. Finally, cover slips were dried and covered with Vectashield HardSet antifade mounting medium (Vector Laboratories, Burlingame, California, USA) and analyzed under a microscope (TCS SP5, Leica, Wetzlar, Germany, objective: HCX PL APO CS 63.0 × 1.40 OIL).

2.6. Quantitative analysis of γH2AX formation

Phosphorylation of H2AX was quantitatively analyzed using an in-cell Western assay modified after Audebert et al. (2010): 2×10^5 cells/well were seeded in a 96-well plate and cultivated for 1 day. Afterwards, cells were treated with 1–500 µM lasiocarpine or with the positive controls doxorubicin (0.25 µM) or aflatoxin B1 (0.1–1 µM). The supernatant was removed after 24 h of incubation, cells were fixed and treated with primary and secondary antibody as described for qualitative analysis of γH2AX formation in section 2.5. However, instead of the treatment with SYTOX Orange nucleic acid stain, cells were incubated for 30 min with DAPI (50 µL/well, 3 µM in PBS) for DNA quantification (compare section 2.4). Finally, fluorescence intensity was measured on a Tecan Infinite M200Pro spectrophotometer (γH2AX: 620Ex/655 Em, DAPI: 380Ex/460 Em). The γH2AX signal was evaluated independently and additionally after normalization to the DNA content as analyzed by DAPI.

2.7. V79 micronucleus test

To assess the human CYP3A4-dependent activation of lasiocarpine towards genotoxic metabolites an *in vitro* mammalian cell micronucleus test was performed with V79-wt and V79-hCYP3A4 cells according to OECD Guideline 487. Thus, 1.6×10^5 cells were seeded on a microscope slide and treated after 1 day of cultivation for 24 h with 0.0001–500 µM lasiocarpine. Vehicle control was 0.2% ACN. Ethyl methanesulfonate (EMS, 350 µg/mL) served as a metabolism-independent positive control. Aflatoxin B1 was used as a metabolism-dependent positive control at a concentration of 1 µM. The experiment was performed under addition of cytochalasin B during incubation. Cytochalasin B is a cytokinesis inhibitor that leads to formation of binuclear cells. Hence cells that underwent mitosis can be identified and differentiated from cells which did not. Treatment medium was removed after 24 h of incubation and cells were subjected to hypertonic treatment with 1.5% sodium citrate solution for 5 min prior to fixation using 0.4% formaldehyde in ethanol acidified with 25% acetic acid. Microscope slides were air-dried before staining with 2.5% of Giemsa solution (Merck, Darmstadt, Germany) in buffer solution according to Weise (Merck, Darmstadt, Germany) and May-Grünwald's eosine-methylene blue solution (modified, Merck). A total of 2000 binuclear cells (1000 binuclear cells per microscope slide) were analyzed for micronuclei under a light microscope at 400× magnification. Only binuclear cells were used for analysis; mono- and polynuclear cells were not included. Structures were recognized as micronuclei if the following criteria were fulfilled: The area counts maximal 30% of the nucleus; staining is similar to the nucleus; they are clearly separated from the nucleus; they show complete cytoplasm.

The cytokinesis block proliferation index (CBPI) was calculated according as followed to assess cytostasis of the treatment. A CBPI of 1 means 100% cytostasis. CBPI values of treated cells should be at least 0.5- to 0.6-fold of the control cells.

$$CBPI = [(N_M) + (2 \times N_B) + (3 \times N_P)] / N_{total}$$

N_M: number of mononuclear cells
N_B: number of binuclear cells
N_P: number of polynuclear cells
N_{total}: total number of cells

2.8. Statistical analysis

Statistically significant differences in multi-comparison procedures with one variable (e.g. concentration series or different supersomes) were calculated by one-way analysis of variance (ANOVA) followed by Dunnett's post-hoc test versus the corresponding control. Scenarios considering two variables (e.g. ketoconazole in a concentration or time series) were analyzed by two-way ANOVA followed by the Holm-Sidak post-hoc test as pairwise multiple comparison procedure. In the micronucleus test, statistically significant different micronucleus formation was analyzed by X^2-test. Dose-dependence of the micronucleus test was analyzed by the Cochran Armitage-trend test using Benchmark Dose Software, U.S. EPA. Results outside of the distribution of the historical negative control data were determined using Poisson-based 95% control limits. Results were considered as significant at $p < 0.05$ and are indicated in the graphs by asterisks: *$p < 0.05$, **$p < 0.01$, ***$p < 0.001$.

3. Results

3.1. In vitro metabolism

3.1.1. CYP quantification and in vitro metabolism of lasiocarpine using liver fractions of rat and human

The total CYP contents of the subcellular liver fractions as determined by measurement of CO-difference spectra are summarized in Table 2.

The *in vitro* metabolism of lasiocarpine provoked a time-dependent decrease in non-metabolized lasiocarpine (Fig. 2) for all tested liver fractions. The rate of metabolism was different between the individual liver fractions: iRS9 and rLM showed the strongest effect, which led to a nearly complete disappearance of lasiocarpine within 1 h. In the presence of nRS9 and hLM lasiocarpine was completely vanished after 2 h of incubation. hS9 showed the weakest degradation with about 60% remaining lasiocarpine after 4.5 h. After addition of 8 μM ketoconazole, a potent CYP3A/Cyp3a inhibitor, metabolism rate significantly decreased for all liver fractions, suggesting that enzymes of the CYP3A/Cyp3a family of human and rat might be involved in lasiocarpine metabolism.

Table 2
Total CYP content of subcellular liver fractions as determined by measurement of CO-difference spectra.

	CYP concentration[pmol/mg protein]
iRS9	651 ± 75
nRS9	236 ± 24
hS9	64 ± 18
rLM	498[a]
	610[b]
hLM	374[a]
	400[b]

[a] Analyzed in one experiment, all other samples were analyzed in triplicates.
[b] According to the manufacturer's specifications.

3.1.2. In vitro metabolism using recombinant human and rat supersomes

Supersomes containing individual human or rat CYP forms were analyzed for their potential to metabolize lasiocarpine in order to identify specific CYP forms involved in the metabolism of lasiocarpine. The results depicted in Fig. 3 show a significant reduction of lasiocarpine only for the human enzymes CYP3A4 and CYP3A5, and for the rat enzymes Cyp3a1 and Cyp3a2. Human CYP3A isoforms caused a decrease down to 13% (CYP3A4) and 68% (CYP3A5). Rat Cyp3a enzymes decreased the lasiocarpine content down to approximately 40%. All other tested supersomes did not significantly alter the lasiocarpine content.

3.2. Cell viability analysis

The cell viability of metabolic incompetent V79-wt cells was compared to V79 stably transfected with human CYP3A4 after lasiocarpine treatment in order to identify the role of human CYP3A4 in regard to lasiocarpine cytotoxicity. Cell viability of V79-wt cells was not altered by lasiocarpine treatment in the DAPI assay (Fig. 4A). The CTB assay showed a statistically significant, but modest decrease in cell viability of V79-wt cells. However, cell viability > 90% was observed in all treatment groups. By contrast, V79-hCYP3A4 cells showed a concentration-dependent decrease in cell viability down to 50% for the highest tested concentration (500 μM) of lasiocarpine (Fig. 4B) in both assays. Experiments with the potent CYP3A inhibitor ketoconazole showed that sensitivity of V79-hCYP3A4 cells towards lasiocarpine is indeed CYP3A4-dependent: coincubation with ketoconazole resulted in statistically significant higher cell viabilities of V79-hCYP3A4, as analyzed by DAPI, compared to treatment without ketoconazole (71% vs. 49% for 500 μM lasiocarpine, Fig. 4C). Incubation with 5 μM ketoconazole alone showed no cytotoxic effect (data not shown).

3.3. Qualitative microscopic analysis of γH2AX formation

The phosphorylation of the histone H2AX (γH2AX formation) can be used as a surrogate for DNA double-strand breaks resulting from exposure to genotoxic compounds. In order to analyze a potential activation of lasiocarpine into genotoxic metabolites, γH2AX formation was analyzed in different variants of the V79 cell line with (V79-hCYP3A4) or without (V79-wt) expression of human CYP3A4. Immunostaining and microscopic observation of γH2AX formation showed no staining of γH2AX after lasiocarpine or aflatoxin B1 treatment in V79-wt cells (Fig. 5). Only treatment with the metabolism-independent positive control doxorubicin resulted in a clear staining of γH2AX. By contrast, staining of γH2AX in lasiocarpine-treated V79-hCYP3A4 resulted in a concentration-dependent increase in the fluorescence intensity. Both positive controls, aflatoxin B1 and doxorubicin, led to staining of γH2AX. These results show a human CYP3A4-dependent phosphorylation of H2AX after lasiocarpine treatment, which can occur after DNA double strand breaks.

3.4. Quantitative analysis of γH2AX formation

The cellular ELISA for γH2AX formation quantitatively verified the results of the microscopic observation. Lasiocarpine treatment showed no effect in V79-wt cells (Fig. 6), while leading to an increased phosphorylation of H2AX in V79-hCYP3A4 cells. The increasing γH2AX signal was observed along with simultaneously decreasing cell counts in V79-hCYP3A4 cells. The γH2AX signal decreased again at high lasiocarpine concentrations, probably due to overbalancing cytotoxicity. Normalization of the γH2AX signal to the respective DNA content clarified the induction of γH2AX formation: clear phosphorylation of H2AX up to 170% compared to solvent control was observed for treatment with lasiocarpine at concentrations of 50 μM or more.

Doxorubicin as a metabolism-independent control for H2AX phosphorylation resulted in comparable signals in V79-wt and V79-

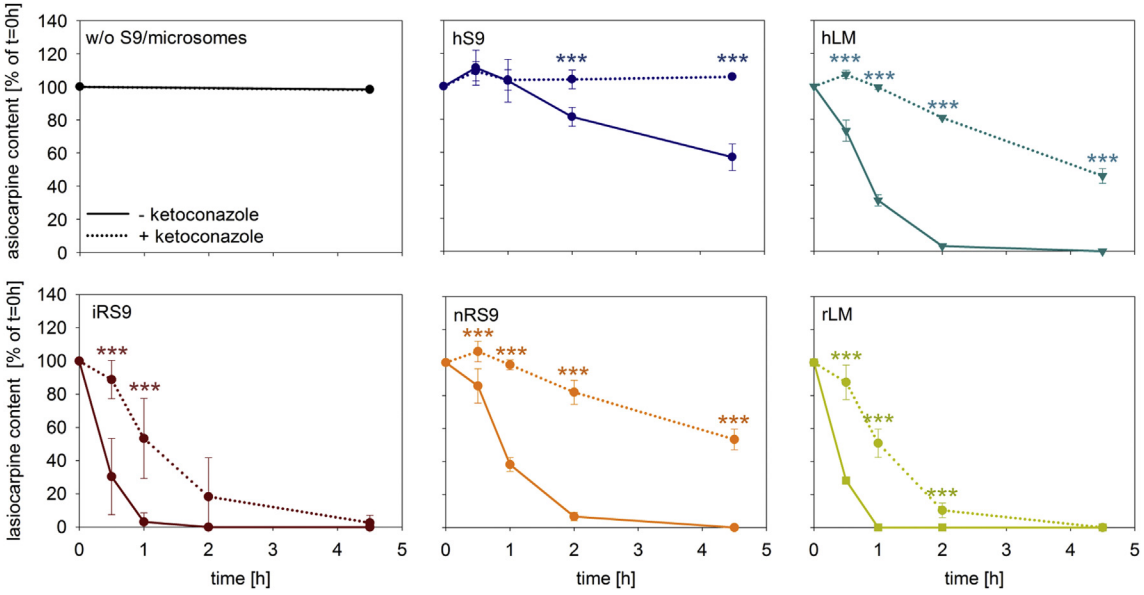

Fig. 2. Time-dependent degradation of lasiocarpine in the presence of different liver fractions of rat or human. Lasiocarpine (10 μM) was incubated with the S9 mix of an induced rat (iRS9), native rat (nRS9) or human (hS9) or with liver microsomes of a native rat (rLM) or human (hLM) without (solid line) or with 8 μM of the potent CYP3A/Cyp3a inhibitor ketoconazole (dotted line). Samples were taken after 0.5, 1, 2 and 4.5 h and analyzed for their content of lasiocarpine by LC-MS/MS. Lasiocarpine content (referred to t = 0 h, set to 100%) is shown as mean ± SD of three separate experiments. Statistically significant differences between the two incubation scenarios with and without ketoconazole in the time series were analyzed by two-way ANOVA followed by Holm-Sidak test as pairwise multiple comparison procedure (***p < 0.001).

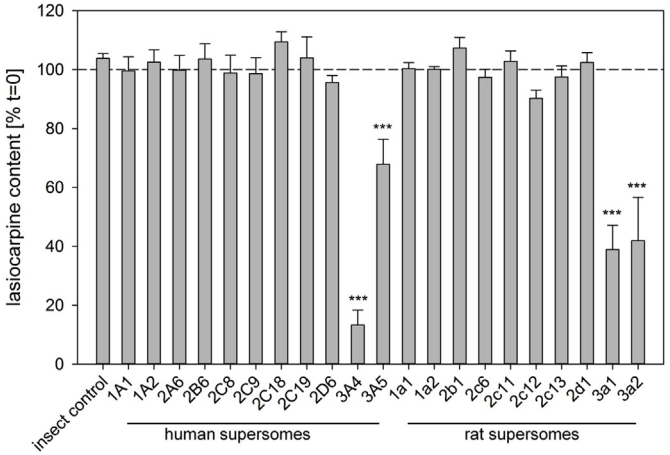

Fig. 3. Reduction of lasiocarpine content by different CYP enzymes of rat and human. A total of 10 μM lasiocarpine was incubated for 4.5 h with different supersomes of rat or human and analyzed for the content of lasiocarpine by LC-MS/MS. Lasiocarpine content (referred to t = 0 h, set to 100%) is shown as mean ± SD of three separate experiments. Significant differences to t = 0 h were calculated by one-way ANOVA followed by Dunnett's post hoc-test (***p < 0.001).

hCYP3A4 (175% and 195%, respectively). Aflatoxin B1 as a metabolism-dependent positive control induced, as expected, effects only in V79-hCYP3A4 (up to 217%). The raw value of the γH2AX signal decreased at high concentrations of aflatoxin B1 with simultaneously decreasing cell counts similar to high lasiocarpine concentrations.

3.5. V79 micronucleus test

The CYP3A4-dependent formation of micronuclei was elucidated as a further endpoint for the induction of DNA damage by lasiocarpine. In V79-wt cells, no micronucleus induction was observed after treatment with 0.1–500 μM lasiocarpine (Fig. 7 and supplementary data Table S1). Number of micronucleus positive cells (MN) per 1000 cells was in the same range for lasiocarpine-treated cells compared to solvent-treated cells (19–26 MN/1000 cells compared to 24–25 MN/1000 cells). By contrast, V79-hCYP3A4 cells showed a concentration-dependent formation of micronuclei reaching statistical significance at 0.1 μM lasiocarpine (20 MN/1000 cells in solvent-treated cells, 19–30 MN/1000 cells for 0.0001–0.01 μM lasiocarpine, 40–56 MN/1000 cells for 0.1–100 μM lasiocarpine, Fig. 7). The number of MN/1000 cells for 0.1 μM lasiocarpine was close to the maximal effect, possibly indicating effect saturation. Higher lasiocarpine concentrations also showed CYP3A4-dependent micronucleus formation. These results are summarized in supplementary data, Table S1. According to OECD guideline no. 487 about the *in vitro* mammalian cell micronucleus test lasiocarpine yielded a clearly positive result in V79-hCYP3A4 cells: at least one of the test concentrations exhibited a statistically significant increase compared with the concurrent negative control, the increase was concentration-related in at least one experimental condition when evaluated with an appropriate trend test, and the results were outside the distribution of historical negative control data (Poisson-based 95% control limits). For V79-wt cells none of these criteria is positive and therefore lasiocarpine is clearly negative in this cell line. Hence, a clear human CYP3A4-dependent induction of micronucleus formation was observed. Treatment with EMS as a metabolism-independent positive control resulted in the induction of micronucleus formation in both cell lines with 34 and 35 MN/1000 cells compared to 24 and 20 MN/1000 cells in the solvent control. Aflatoxin B1 as a metabolism-dependent positive control clearly induced micronuclei in the V79-hCYP3A4 cells. V79-wt cells were negative for micronucleus induction by aflatoxin B1.

The CBPI (supplementary data Table S1) was not influenced by lasiocarpine in V79-wt cells whereas V79-hCYP3A4 cells showed a concentration-dependent decreasing CBPI after lasiocarpine treatment. This is indicative of an impairment of proliferation by bioactivated lasiocarpine.

4. Discussion

In this study, we compared the metabolic elimination of the PA

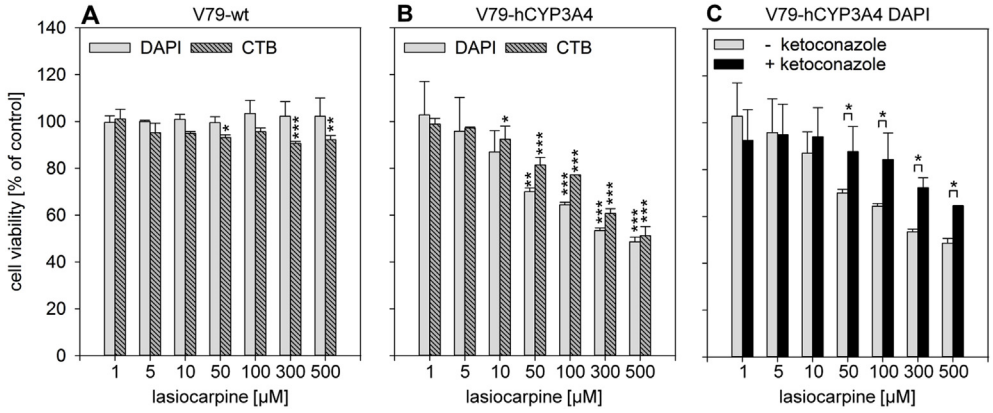

Fig. 4. Cell viability of V79-wt (A) and V79-hCYP3A4 (B) cells after 24 h lasiocarpine treatment as determined by DAPI (light gray bars) and CellTiter-Blue viability assay (CTB; dark gray, striped bars). Cell viability of V79-hCYP3A4 cells after treatment with lasiocarpine alone (gray bars) or co-treatment with 5 µM of the potent CYP3A inhibitor ketoconazole (black bars) as analyzed by DAPI is also shown (C). Results are given as mean ± SD of three separate experiments, each conducted in triplicates. Statistically significant differences in the lasiocarpine concentrations series were calculated by one-way ANOVA followed by Dunnett's post-hoc test. Statistically significant differences between the two incubation scenarios with and without ketoconazole in the concentration series were analyzed by two-way ANOVA followed by Holm-Sidak test as pairwise multiple comparison procedure. Results are indicated by asterisks: *$p < 0.05$, **$p < 0.01$, ***$p < 0.001$.

lasiocarpine in the presence of subcellular liver fractions of rat and human. Enzymes from both species led to a reduction of the lasiocarpine content in the incubation mixture, but at different turnover rates. Our results are in line with previous studies: Kolrep et al. (2018) observed a clear degradation of lasiocarpine by rat S9 fraction while human S9 fractions showed only slight metabolic degradation of lasiocarpine. In our study, the differences observed in the effect strength appear to be due to differences in the CYP contents of different liver fractions: higher turnover rates were observed for microsomes as compared to S9 fractions, for induced S9 fraction, as compared to native S9 fraction and for human fractions, as compared to rat fractions. Microsomes in general contain higher levels of CYPs per mg protein than S9 fraction due to the separation of the cytosolic fraction from the microsomal fraction during production. Induced S9 fraction contains higher levels of CYPs than the native S9 fraction due to treatment with the CYP inducers β-naphthoflavone and phenobarbital (Omiecinski et al., 1999; Parkinson, 1996). Total CYP content of the human liver was shown to be significantly lower than total CYP content of the rat liver (Hrycay and Bandiera, 2008). This is supported by the results of the total CYP quantification by CO-difference spectra measurements. The strength of the turnover rate correlates with the total CYP content of the subcellular liver fractions. The varying CYP composition or varying catalytic activity (Martignoni et al., 2006; Taneja et al., 2018) might be further reasons for differences in the turnover rate observed in our experiments. Other authors have stated before that human S9 fraction is not always the most active and best *in vitro* system to analyze metabolism-dependent toxicity of xenobiotics (Cox et al., 2016; Nesslany, 2017).

The addition of the potent CYP3A/Cyp3a inhibitor ketoconazole to the incubation mixtures resulted in reduction of lasiocarpine conversion under all incubation conditions, suggesting that enzymes of the CYP3A/Cyp3a family are of major relevance for lasiocarpine metabolism in both species, rat and human. As ketoconazole inhibits CYP3A enzymes selectively amongst human enzymes in the concentration range used (Eagling et al., 1998), lasiocarpine metabolism could be directly attributed to this human enzyme class. In rat liver homogenates, ketoconazole is a potent Cyp3a inhibitor, but inhibits also reactions mediated by other enzymes (Eagling et al., 1998). Hence, inhibition of

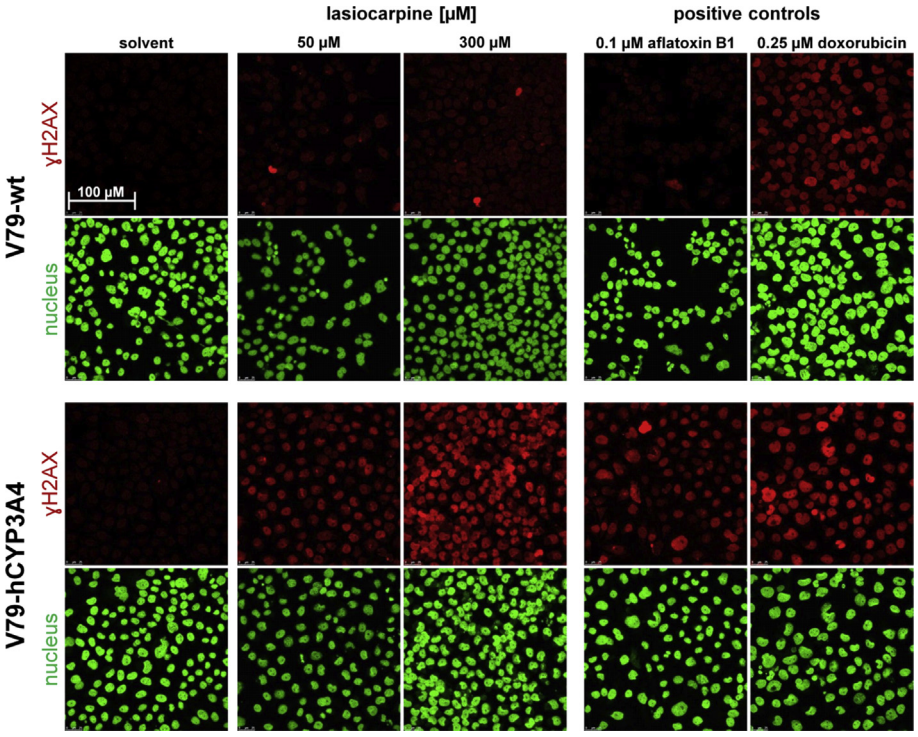

Fig. 5. Phosphorylation of the histone H2AX after 24 h of treatment with lasiocarpine, the metabolism-dependent positive control aflatoxin B1, or the metabolism-independent positive control doxorubicin. γH2AX was stained with a combination of primary anti-γH2AX and secondary Alexa Fluor 633-antibody and is shown in red. Nuclei were stained using SYTOX Orange nucleic acid stain and are displayed in green. Brightness was increased by 30% for all microscope images. (For interpretation of the references to colour in this figure legend, the reader is referred to the Web version of this article.)

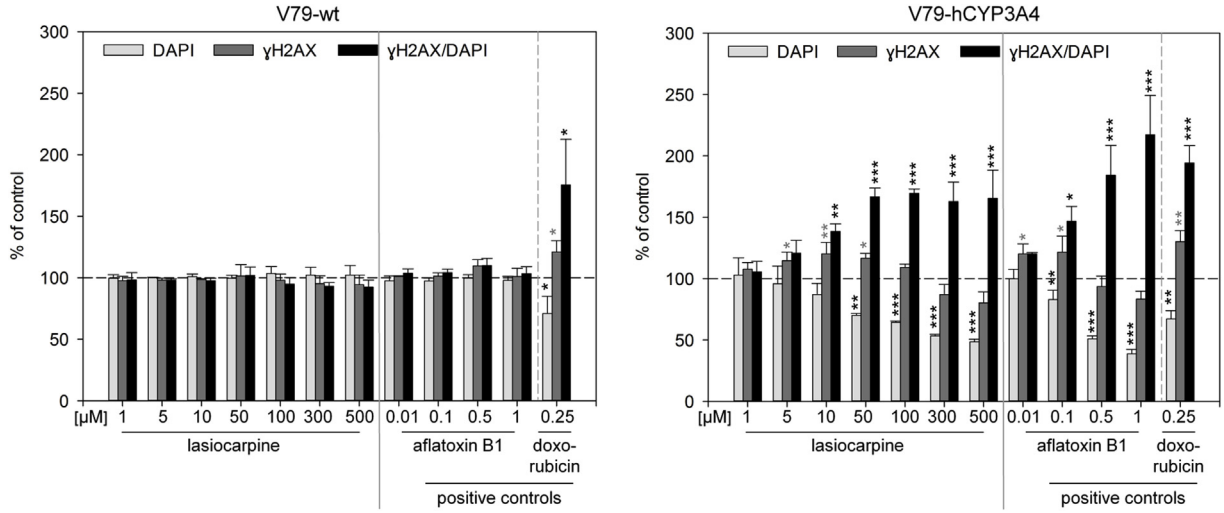

Fig. 6. γH2AX formation and cell viability as analyzed by DNA quantification via DAPI staining (light gray) in V79-wt and V79-hCYP3A4 cells after 24 h of treatment with lasiocarpine, the metabolism-dependent positive control aflatoxin B1, or the metabolism-independent positive control doxorubicin. γH2AX results are shown as raw values (dark gray) and after normalization to the corresponding DNA content (black). Results are given as mean ± SD of three separate experiments, each conducted in triplicates. Significant differences versus the respective solvent control [0.2% ACN, set to 100% (dashed line)] were calculated by one-way ANOVA followed by Dunnett's post-hoc test (*p < 0.05, **p < 0.01, ***p < 0.001).

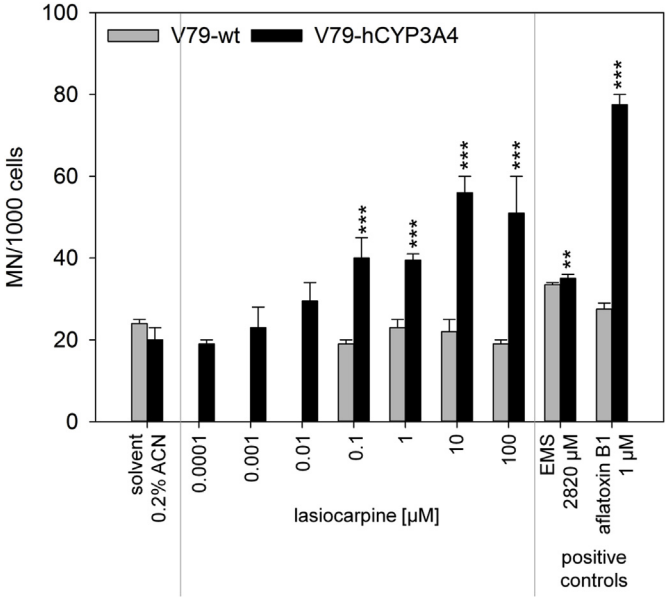

Fig. 7. Micronucleus formation in V79-wt (gray bars) and V79-hCYP3A4 cells (black bars) after 24 h of treatment with lasiocarpine, the metabolism-dependent positive control aflatoxin B1, or the metabolism-independent positive control ethyl methanesulfate (EMS). Numbers of micronucleus positive cells (MN) per 1000 analyzed cells are shown as mean ± half range of duplicates from one experiment. Statistically significant differences vs. the respective solvent control were calculated by X^2-test (**p < 0.01, ***p < 0.001). Detailed results of this experiment and further experiments covering a different concentration range including calculated CBPI values are summarized in supplementary data Table S1.

lasiocarpine metabolism in rat systems by ketoconazole might have been also caused by inhibition of CYP forms other than members of the Cyp3a subfamily. The role of CYP3A/Cyp3a in lasiocarpine metabolism was therefore verified by experiments using supersomes. The observation of Cyp3a-mediated metabolism of lasiocarpine is in line with results from previous studies which reported that Cyp3a enzymes in rodents lead to an activation of PA (Fu et al., 2004; Kasahara et al., 1997; Reid et al., 1998). A few studies also showed activation of other PA by human CYP3A4 before. Miranda et al. (1991) and Xia et al. (2003) showed formation of electrophilic pyrrolic intermediates after incubation with human liver microsomes, which was inhibited by addition of the CYP3A4 inhibitor triacetyloleandomycin. Ruan et al. (2014) showed CYP3A4-mediated pyrrole-glutathione adduct formation for lasiocarpine and other PA in experiments with supersomes. Dai et al. (2010) presented similar findings for the PA monocrotaline and retrorsine. Glutathione was used as a scavenger of the electrophilic reactive intermediate of PA. This analysis did not show directly a toxic potential of the PA metabolites. Conversion towards cytotoxic metabolites by human CYP3A4 was shown by Tu et al. (2014) for the PA retrorsine in experiments with a human CYP3A4-expressing clone of MDCK cells. However, the authors did not analyze the molecular mechanisms of toxicity. Our study with human CYP3A4-expressing V79 cells confirms the results of Tu et al. for lasiocarpine and offers deeper insights into CYP3A4-dependent molecular mechanisms: we show genotoxicity as a mechanism of CYP3A4-dependent toxicity. In our experiments, phosphorylation of the histone H2AX, which is associated with DNA double-strand breaks, was observed only after lasiocarpine activation by CYP3A4. This points towards a CYP3A4-dependent genotoxic potential of PA, but is no direct evidence for genotoxicity as phosphorylation of H2AX may also occur in the context of other cellular events such as apoptosis (Rogakou et al., 2000) or in mitotic cells in the absence of DNA damage (An et al., 2010; McManus and Hendzel, 2005; Tu et al., 2013). The apoptotic potential of PA has been shown before (Copple et al., 2004; Ji et al., 2008; Liu et al., 2017; Waizenegger et al., 2018). However, CYP3A4-dependence of this phosphorylation was clearly shown within our study.

Direct evidence for the conversion of lasiocarpine to genotoxic metabolites by human CYP3A4 is provided by our results from the micronucleus assay. Induction of micronuclei was observed only in V79-hCYP3A4 cells but not in V79-wt cells. The genotoxic potential of different PA has been shown before: Allemang et al. (2018) observed micronucleus induction by different PA in the metabolically competent cell line HepaRG. For lasiocarpine, they observed statistically significant induction of micronuclei starting from a concentration of 0.59 μM, which is in the same order of magnitude as the lasiocarpine concentrations leading to micronucleus induction in our experiments. However, due to the use of a metabolically competent cell line the authors from the above study could not distinguish between metabolism-independent and metabolism-dependent effects. Metabolism-

dependence of the clastogenic potential of PA was shown by Müller et al. (1992) by analysis of chromosomal aberrations in V79 cells treated with the PA retrorsine, monocrotaline and isatidine without and with bioactivation with Aroclor-induced rat S9 mix or primary rat hepatocytes. They observed an increased clastogenic potential for bioactivated PA. Our results for the first time directly link the metabolism-dependent genotoxicity of lasiocarpine to a specific human enzyme. It is remarkable, that the human CYP3A4-dependent micronucleus induction occurs in a broad concentration range (0.1–500 µM lasiocarpine).

Another interesting fact is the decreasing CBPI value of lasiocarpine-treated V79-hCYP3A4 cells, which suggests a CYP3A4-dependent impairment of proliferation. A decrease in the CBPI means an increased proportion of mononuclear cells and thus fewer cells which underwent mitosis. This finding is in line with the antimitotic potential described for lasiocarpine, heliotrine and monocrotaline in rat livers (Allen et al., 1975; Culvenor et al., 1969). Mattocks and Legg (1980) extended these antimitotic findings in cultured hepatocytes to dehydroretronecine, a PA metabolite. This finding suggests that the antimitotic potential is another metabolism-dependent effect, which agrees with our results of a decreasing CBPI only for CYP3A4-activated lasiocarpine.

It has been reported that p53-deficient cell lines such as V79 are susceptible for giving misleading positive results in the micronucleus assay, which means positive results for substances that do not show DNA reactivity or genotoxicity *in vivo* (Fowler et al., 2012). As micronucleus induction was also observed after PA treatment *in vivo* (Sanderson and Clark, 1993; Takashima et al., 2015) and lasiocarpine was shown to form DNA adducts after activation by rat liver microsomes (Xia et al., 2006), there is convincing evidence that the positive response in our experiments is not an artifact. However, it has to be mentioned that our *in vitro* model is an artificial system to analyze the CYP3A4-dependent toxicity of lasiocarpine. While some glutathione *S*-transferase activities are very high in V79 cells (Glatt et al., 1990), other potentially detoxifying enzymes may not be contained or functional in that system. Metabolism of PA is known to comprise activating as well as detoxifying reactions and susceptibility towards PA toxicity is assumed to be based on the relative activity of these two reaction types (Wiedenfeld et al., 2008). This balance may be different in the human liver as compared to the experimental model used.

In summary, our results demonstrate that both analyzed species, rat and human, are able to metabolize the PA representative lasiocarpine in both liver fractions, S9 and microsomes. The rate of lasiocarpine conversion is suggested to be based on the CYP content/activity. Enzymes of the CYP3A/Cyp3a family were identified as key enzymes for lasiocarpine metabolism. Human CYP3A4 is capable of toxifying the PA representative lasiocarpine confirming previous results from the literature. We elucidated for the first time a direct link that formation of genotoxic metabolites is mediated by human CYP3A4. Hence we conclude, that it is essential to consider metabolism of PA for human risk assessment.

Conflicts of interest

The authors declare that there are no conflicts of interest.

Acknowledgements

This work was supported by the German Research Foundation (grant number LA1177/12-1) and by the German Federal Institute for Risk Assessment (grant numbers 1322-591 and 1322-624). Prof. Dr. Vlada B. Urlacher and Sebastian Hölzel are acknowledged for their support with the CYP quantification. Furthermore, we thank Inga Mädge for her support with the LC-MS/MS measurements and Anja Koellner and Marlies Sagmeister for skillful technical assistance.

Transparency document

Transparency document related to this article can be found online at https://doi.org/10.1016/j.fct.2019.05.019

Appendix A. Supplementary data

Supplementary data to this article can be found online at https://doi.org/10.1016/j.fct.2019.05.019.

References

Allemang, A., Mahony, C., Lester, C., Pfuhler, S., 2018. Relative potency of fifteen pyrrolizidine alkaloids to induce DNA damage as measured by micronucleus induction in HepaRG human liver cells. Food Chem. Toxicol. 121, 72–81.
Allen, J.R., Hsu, I.C., Carstens, L.A., 1975. Dehydroretronecine-induced rhabdomyosarcomas in rats. Cancer Res. 35, 997–1002.
Ames, B.N., McCann, J., Yamasaki, E., 1975. Methods for detecting carcinogens and mutagens with the salmonella/mammalian-microsome mutagenicity test. Mutat. Res. 31, 347–363.
An, J., Huang, Y.-C., Xu, Q.-Z., Zhou, L.-J., Shang, Z.-F., Huang, B., Wang, Y., Liu, X.-D., Wu, D.-C., Zhou, P.-K., 2010. DNA-PKcs plays a dominant role in the regulation of H2AX phosphorylation in response to DNA damage and cell cycle progression. BMC Mol. Biol. 11, 18.
Audebert, M., Riu, A., Jacques, C., Hillenweck, A., Jamin, E.L., Zalko, D., Cravedi, J.P., 2010. Use of the gammaH2AX assay for assessing the genotoxicity of polycyclic aromatic hydrocarbons in human cell lines. Toxicol. Lett. 199, 182–192.
Baldwin, S.J., Bloomer, J.C., Smith, G.J., Ayrton, A.D., Clarke, S.E., Chenery, R.J., 1995. Ketoconazole and sulphaphenazole as the respective selective inhibitors of P4503A and 2C9. Xenobiotica 25, 261–270.
BfR, 2013. Pyrrolizidine alkaloids in herbal teas and teas. BfR Opinion No 018/2013, 1–31.
BfR, 2016. Pyrrolizidine alkaloids: levels in foods should continue to be kept as low as possible. BfR Opinion No 030/2016, 1–53.
BfR, 2018. Updated risk evaluation of levels of 1,2-unsaturated pyrrolizidine alkaloids (PA) in foods. BfR Opinion No 020/2018, 1–13.
Bodi, D., Ronczka, S., Gottschalk, C., Behr, N., Skibba, A., Wagner, M., Lahrssen-Wiederholt, M., Preiss-Weigert, A., These, A., 2014. Determination of pyrrolizidine alkaloids in tea, herbal drugs and honey. Food Addit. Contam. A 31, 1886–1895.
Bradford, M.M., 1976. A rapid and sensitive method for the quantitation of microgram quantities of protein utilizing the principle of protein-dye binding. Anal. Biochem. 72, 248–254.
Chen, T., Mei, N., Fu, P.P., 2010. Genotoxicity of pyrrolizidine alkaloids. J. Appl. Toxicol. 30, 183–196.
Copple, B.L., Rondelli, C.M., Maddox, J.F., Hoglen, N.C., Ganey, P.E., Roth, R.A., 2004. Modes of cell death in rat liver after monocrotaline exposure. Toxicol. Sci. 77, 172–182.
Cox, J.A., Fellows, M.D., Hashizume, T., White, P.A., 2016. The utility of metabolic activation mixtures containing human hepatic post-mitochondrial supernatant (S9) for in vitro genetic toxicity assessment. Mutagenesis 31, 117–130.
Culvenor, C.C.J., Downing, D.T., Edgar, J.A., Jago, M.V., 1969. Pyrrolizidine alkaloids as alkylating and antimitotic agents. Ann. N. Y. Acad. Sci. 163, 837–847.
Dai, J., Zhang, F., Zheng, J., 2010. Retrorsine, but not monocrotaline, is a mechanism-based inactivator of P450 3A4. Chem. Biol. Interact. 183, 49–56.
Dusemund, B., Nowak, N., Sommerfeld, C., Lindtner, O., Schafer, B., Lampen, A., 2018. Risk assessment of pyrrolizidine alkaloids in food of plant and animal origin. Food Chem. Toxicol. 115, 63–72.
Eagling, V.A., Tjia, J.F., Back, D.J., 1998. Differential selectivity of cytochrome P450 inhibitors against probe substrates in human and rat liver microsomes. Br. J. Clin. Pharmacol. 45, 107–114.
EFSA, 2005. Opinion of the scientific committee on a request from EFSA related to a harmonised approach for risk assessment of substances which are both genotoxic and carcinogenic. EFSA Journal 3, 282.
EFSA, 2011. Scientific opinion on pyrrolizidine alkaloids in food and feed - EFSA panel on contaminants in the food chain (CONTAM). EFSA Journal 9, 2406.
EFSA, 2017. Risks for human health related to the presence of pyrrolizidine alkaloids in honey, tea, herbal infusions and food supplements - EFSA panel on contaminants in the food chain (CONTAM). EFSA Journal 15, 4908.
Fowler, P., Smith, K., Young, J., Jeffrey, L., Kirkland, D., Pfuhler, S., Carmichael, P., 2012. Reduction of misleading ("false") positive results in mammalian cell genotoxicity assays. I. Choice of cell type. Mutat. Res. 742, 11–25.
Fu, P.P., Xia, Q., Lin, G., Chou, M.W., 2004. Pyrrolizidine alkaloids - genotoxicity, metabolism enzymes, metabolic activation, and mechanisms. Drug Metab. Rev. 36, 1–55.
Glatt, H., Gemperlein, I., Setiabudi, F., Platt, K.L., Oesch, F., 1990. Expression of xenobiotic-metabolizing enzymes in propagatable cell cultures and induction of micronuclei by 13 compounds. Mutagenesis 5, 241–249.
He, X., Xia, Q., Fu, P.P., 2017. 7-Glutathione-pyrrole and 7-cysteine-pyrrole are potential carcinogenic metabolites of pyrrolizidine alkaloids. J. Environ. Sci. Health C Environ. Carcinog. Ecotoxicol. Rev. 35, 69–83.
Hrycay, E.G., Bandiera, S.M., 2008. Cytochrome P450 enzymes. In: Gad, S.C. (Ed.), Preclinical Development Handbook - ADME and Biopharmaceutical Properties. John

Wiley and Sons, Inc., Hoboken, New Jersey, pp. 627–696.
Ji, L., Chen, Y., Liu, T., Wang, Z., 2008. Involvement of Bcl-xL degradation and mitochondrial-mediated apoptotic pathway in pyrrolizidine alkaloids-induced apoptosis in hepatocytes. Toxicol. Appl. Pharmacol. 231, 393–400.
Ji, L., Liu, T., Chen, Y., Wang, Z., 2009. Protective mechanisms of N-acetyl-cysteine against pyrrolizidine alkaloid clivorine-induced hepatotoxicity. J. Cell. Biochem. 108, 424–432.
Kakar, F., Akbarian, Z., Leslie, T., Mustafa, M.L., Watson, J., Van Egmond, H.P., Omar, M.F., Mofleh, J., 2010. An outbreak of hepatic veno-occlusive disease in Western Afghanistan associated with exposure to wheat flour contaminated with pyrrolizidine alkaloids. J. Toxicol. 2010 Article ID 313280.
Kasahara, Y., Kiyatake, K., Tatsumi, K., Sugito, K., Kakusaka, I., Yamagata, S., Ohmori, S., Kitada, M., Kuriyama, T., 1997. Bioactivation of monocrotaline by P-450 3A in rat liver. J. Cardiovasc. Pharmacol. 30, 124–129.
Kolrep, F., Numata, J., Kneuer, C., Preiss-Weigert, A., Lahrssen-Wiederholt, M., Schrenk, D., These, A., 2018. In vitro biotransformation of pyrrolizidine alkaloids in different species. Part I: microsomal degradation. Arch. Toxicol. 92, 1089–1097.
Liu, W., Li, X., Zhou, B., Fang, S., Ho, W., Chen, H., Liang, H., Ye, L., Tang, J., 2017. Differential induction of apoptosis and autophagy by pyrrolizidine alkaloid clivorine in human hepatoma Huh-7.5 cells and its toxic implication. PLoS One 12, e0179379.
Liu, Y., Hu, K., Jia, H., Jin, G., Glatt, H., Jiang, H., 2016. Potent mutagenicity of some non-planar tri- and tetrachlorinated biphenyls in mammalian cells, human CYP2E1 being a major activating enzyme. Arch. Toxicol. 1–14.
Martignoni, M., Groothuis, G.M.M., de Kanter, R., 2006. Species differences between mouse, rat, dog, monkey and human CYP-mediated drug metabolism, inhibition and induction. Expert Opin. Drug Metabol. Toxicol. 2, 875–894.
Mattocks, A.R., 1986. Relationship between Structure, Metabolism and Toxicity, Chemistry and Toxicology of Pyrrolizidine Alkaloids. pp. 316–329.
Mattocks, A.R., Legg, R.F., 1980. Antimitotic activity of dehydroretronecine, a pyrrolizidine alkaloid metabolite, and some analogous compounds, in a rat liver parenchymal cell line. Chem. Biol. Interact. 30, 325–336.
Maurice, M., Pichard, L., Daujat, M., Fabre, I., Joyeux, H., Domergue, J., Maurel, P., 1992. Effects of imidazole derivatives on cytochromes P450 from human hepatocytes in primary culture. FASEB J. 6, 752–758.
McManus, K.J., Hendzel, M.J., 2005. ATM-dependent DNA damage-independent mitotic phosphorylation of H2AX in normally growing mammalian cells. Mol. Biol. Cell 16, 5013–5025.
Miranda, C.L., Reed, R.L., Guengerich, F.P., Buhler, D.R., 1991. Role of cytochrome P450IIIA4 in the metabolism of the pyrrolizidine alkaloid senecionine in human liver. Carcinogenesis 12, 515–519.
Mulder, P.P.J., López, P., Castelari, M., Bodi, D., Ronczka, S., Preiss-Weigert, A., These, A., 2018. Occurrence of pyrrolizidine alkaloids in animal- and plant-derived food: results of a survey across Europe. Food Addit. Contam. A 35, 118–133.
Müller, L., Kasper, P., Kaufmann, G., 1992. The clastogenic potential in vitro of pyrrolizidine alkaloids employing hepatocyte metabolism. Mutat. Res. 282, 169–176.
Nesslany, F., 2017. The current limitations of in vitro genotoxicity testing and their relevance to the in vivo situation. Food Chem. Toxicol. 106, 609–615.
Neuman, M.G., Jia, A.Y., Steenkamp, V., 2007. Senecio latifolius induces in vitro hepatocytotoxicity in a human cell line. Can. J. Physiol. Pharmacol. 85, 1063–1075.
Omiecinski, C.J., Remmel, R.P., Hosagrahara, V.P., 1999. Concise review of the cytochrome P450s and their roles in toxicology. Toxicol. Sci. 48, 151–156.
Omura, T., Sato, R., 1964. The carbon monoxide-binding pigment of liver microsomes. I. Evidence for ihts hemoprotein nature. J. Biol. Chem. 239, 2370–2378.
Parkinson, A., 1996. Biotransformation of xenobiotics. In: Klaassen, C.D. (Ed.), Casarett & Doull's Toxicology: the Basic Science of Poisons. McGraw-Hill, New York, pp. 113–186.
Prakash, A.S., Pereira, T.N., Reilly, P.E., Seawright, A.A., 1999. Pyrrolizidine alkaloids in human diet. Mutat. Res. 443, 53–67.
Reid, M.J., Lame, M.W., Morin, D., Wilson, D.W., Segall, H.J., 1998. Involvement of cytochrome P450 3A in the metabolism and covalent binding of 14C-monocrotaline in rat liver microsomes. J. Biochem. Mol. Toxicol. 12, 157–166.
Rogakou, E.P., Nieves-Neira, W., Boon, C., Pommier, Y., Bonner, W.M., 2000. Initiation of DNA fragmentation during apoptosis induces phosphorylation of H2AX histone at serine 139. J. Biol. Chem. 275, 9390–9395.
Ruan, J., Yang, M., Fu, P., Ye, Y., Lin, G., 2014. Metabolic activation of pyrrolizidine alkaloids: insights into the structural and enzymatic basis. Chem. Res. Toxicol. 27, 1030–1039.
Sanderson, B.J., Clark, A.M., 1993. Micronuclei in adult and foetal mice exposed in vivo to heliotrine, urethane, monocrotaline and benzidine. Mutat. Res. 285, 27–33.
Schneider, A., Schmalix, W.A., Siruguri, V., de Groene, E.M., Horbach, G.J., Kleingeist, B., Lang, D., Bocker, R., Belloc, C., Beaune, P., Greim, H., Doehmer, J., 1996. Stable expression of human cytochrome P450 3A4 in conjunction with human NADPH-cytochrome P450 oxidoreductase in V79 Chinese hamster cells. Arch. Biochem. Biophys. 332, 295–304.
Takashima, R., Takasawa, H., Wako, Y., Yasunaga, K., Hattori, A., Kawabata, M., Nakadate, K., Nakagawa, M., Hamada, S., 2015. Micronucleus induction in rat liver and bone marrow by acute vs. repeat doses of the genotoxic hepatocarcinogen monocrotaline. Mutat. Res. Genet. Toxicol. Environ. Mutagen 780–781, 64–70.
Tandon, B.N., Tandon, H.D., Tandon, R.K., Narndranathan, M., Joshi, Y.K., 1976. An epidemic of veno-occlusive disease of liver in Central India. The Lancet 308, 271–272.
Taneja, I., Karsauliya, K., Rashid, M., Sonkar, A.K., Rama Raju, K.S., Singh, S.K., Das, M., Wahajuddin, M., Singh, S.P., 2018. Species differences between rat and human in vitro metabolite profile, in vivo predicted clearance, CYP450 inhibition and CYP450 isoforms that metabolize benzanthrone: implications in risk assessment. Food Chem. Toxicol. 111, 94–101.
Tu, M., Li, L., Lei, H., Ma, Z., Chen, Z., Sun, S., Xu, S., Zhou, H., Zeng, S., Jiang, H., 2014. Involvement of organic cation transporter 1 and CYP3A4 in retrorsine-induced toxicity. Toxicology 322, 34–42.
Tu, W.-Z., Li, B., Huang, B., Wang, Y., Liu, X.-D., Guan, H., Zhang, S.-M., Tang, Y., Rang, W.-Q., Zhou, P.-K., 2013. γH2AX foci formation in the absence of DNA damage: mitotic H2AX phosphorylation is mediated by the DNA-PKcs/CHK2 pathway. FEBS Lett. 587, 3437–3443.
Waizenegger, J., Braeuning, A., Templin, M., Lampen, A., Hessel-Pras, S., 2018. Structure-dependent induction of apoptosis by hepatotoxic pyrrolizidine alkaloids in the human hepatoma cell line HepaRG: single versus repeated exposure. Food Chem. Toxicol. 114, 215–226.
Wiedenfeld, H., 2011. Plants containing pyrrolizidine alkaloids: toxicity and problems. Food Addit. Contam. A 28, 282–292.
Wiedenfeld, H., Roeder, E., Bourauel, T., Edgar, J., 2008. Pyrrolizidine Alkaloids - Structure and Toxicity. Verlag V&R Unipress, Bonn.
Xia, Q., Chou, M.W., Edgar, J.A., Doerge, D.R., Fu, P.P., 2006. Formation of DHP-derived DNA adducts from metabolic activation of the prototype heliotridine-type pyrrolizidine alkaloid, lasiocarpine. Cancer Lett. 231, 138–145.
Xia, Q., Chou, M.W., Kadlubar, F.F., Chan, P.C., Fu, P.P., 2003. Human liver microsomal metabolism and DNA adduct formation of the tumorigenic pyrrolizidine alkaloid, riddelliine. Chem. Res. Toxicol. 16, 66–73.